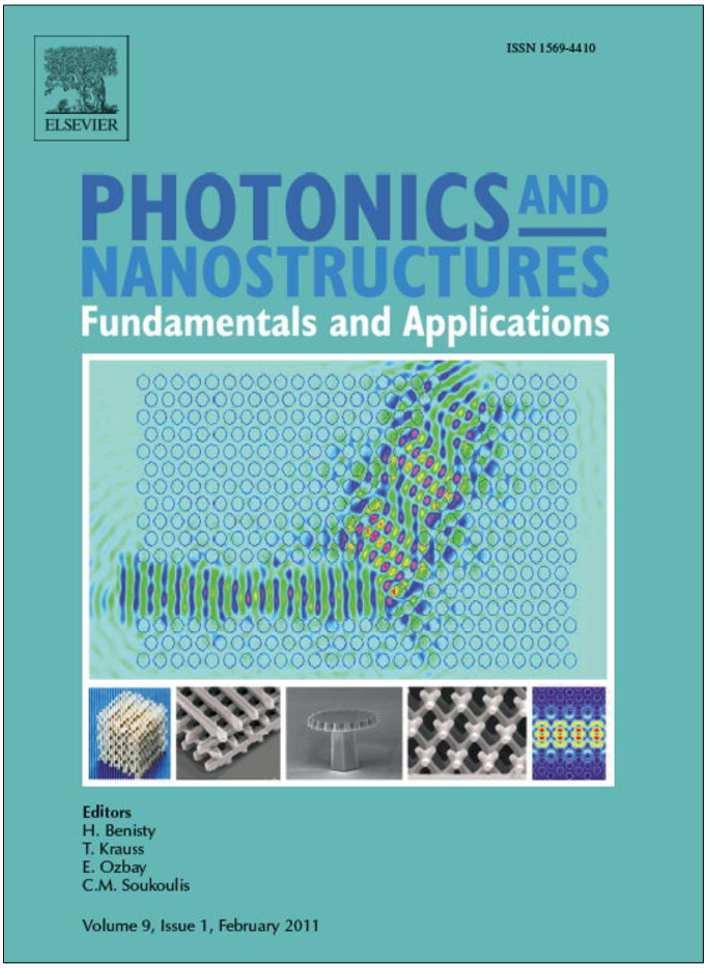
ISSN 1569-4410
ELSEVIER
PHOTONICS AND NANOSTRUCTURES
Fundamentals and Applications
Editors
H. Benisty
T. Krauss
E. Ozbay
C.M. Soukoulis
Volume 9, Issue 1, February 2011

Available online at www.sciencedirect.com

ScienceDirect

ELSEVIER

Photonics and Nanostructures – Fundamentals and Applications 9 (2011) 63–69

PHOTONICS AND NANOSTRUCTURES Fundamentals and Applications

www.elsevier.com/locate/photonics

Q-factor optimization for TM-like modes in pillar-based photonic crystal cavities with planar slot waveguides

D. Mascoli, D. Gerace *, L.C. Andreani

Dipartimento di Fisica "Alessandro Volta," Università degli Studi di Pavia, via Bassi 6, 27100 Pavia, Italy

Received 22 July 2010; received in revised form 20 October 2010; accepted 23 October 2010
Available online 30 October 2010

Abstract

We propose a design for high Q-factor, pillar-based photonic crystal cavities, with the goal of enhancing radiation–matter interaction in planar slot waveguides. The Q-factor is optimized for transverse-magnetic-like (TM-like) cavity modes, and it is found that a maximum $Q \simeq 45000$ can be reached by proper design of the pillars defining the cavity region. As an application, we study the Purcell enhancement of spontaneous emission rate for a dipole emitter within a thin layer of low index material (slot) grown at the pillars center. The field intensity is enhanced within the slot for TM-like modes, which yields a Purcell factor of the order of 10^4, larger than the corresponding structure without slot. These results directly apply to nanostructures made of a thin active layer of erbium-doped silicon dioxide embedded in silicon pillars, which can be readily fabricated with state-of-the art technology.

Keywords: Photonic crystal cavities; Slot waveguides

1. Introduction

Most photonic crystal (PhC) devices are currently designed and realized as means to efficiently manipulate the confinement and propagation of light in all the three spatial dimensions [1], with the aim of realizing both passive and active photonic integrated components. Photonic crystal slabs [2], i.e. two-dimensional (2D) PhCs embedded in planar waveguide geometries, are particularly effective in realizing an efficient three-dimensional (3D) confinement of the electromagnetic field. Photonic cavities with extremely high Q-factors ($Q \sim 10^5$–10^6) together with diffraction limited mode volumes [$V_{\rm eff} \sim (\lambda/n)^3$] have been already demonstrated in such systems [3,4]. The figure of merit represented by $Q/V_{\rm eff}$ is essential in enhancing the radiation–matter coupling of dipolar emitters placed within the cavity [5,6]. The Purcell enhancement (F_P) of spontaneous emission rate [7] has been shown to occur in semiconductor systems with PhC cavities [8–10] based on III–V materials, which is crucial for applications such as low-threshold lasing or single-photon sources.

On the other hand, it would be highly desirable to apply such concepts in the field of silicon (Si) photonics [11], where active devices based on a Si platform are strongly required. Along these lines, enhanced vertical emission [12] and reduction of spontaneous emission lifetime [13] have been experimentally shown, e.g., by using a thin layer of active erbium-doped silica within a waveguide core made of poly-Si in a planar configuration, employing the principle of slot waveguide confinement [14–18]. Using 3D confinement, enhanced F_P factor can be obtained by reducing $V_{\rm eff}$. The

* Corresponding author. Tel.: +39 (0)382 987470.
E-mail addresses: dario.gerace@unipv.it (D. Gerace), lucio.andreani@unipv.it (L.C. Andreani).

1569-4410/$ – see front matter
doi:10.1016/j.photonics.2010.10.001

discontinuity of the normal electric-field component at the interfaces of a low-index slot within a high-index material allows an efficient confinement of the field within the low index, sub-wavelength region, while confinement in the other two directions can be achieved by using a 2D PhC cavity. Thus, combining high-Q PhC cavities and slot confinement is one of the current goals in solid-state cavity quantum electrodynamics (CQED).

For the case of vertical slot waveguides [14,15], which operate with transverse-electric (TE) polarization, different designs have been proposed [19–21] using a PhC lattice made of holes in a dielectric matrix, usually in a suspended membrane. So far, even if planar (horizontal) slot waveguides have been fabricated and characterized [16,17], no work has been devoted to the optimization and realization of PhC cavities in view of CQED applications of such structures. Since such waveguides operate in transverse-magnetic (TM) polarization (i.e. with the electric field mainly perpendicular to the slab plane), the appropriate PhC lattice must be based on pillar structures. We consider high-index pillars embedded in a low-index dielectric medium, typically Si pillars in SiO_2, and these structures have the unequivocal advantage of being self-supported all-dielectric devices, as opposed to suspended membranes. Extended theoretical work has been done on line-defect waveguides in a square lattice of pillars [1,2] and interestingly low propagation losses have been measured in such structures [22,23]. It has also been argued that such pillar-based structures might be less sensitive to disorder-induced losses [24]. Moreover, the technology is quite mature and efficient quantum cascade [25] or vertically emitting [26] lasers based on TM-like modes in pillar based PhC lattices have been realized. Recently, high Q-factors (∼7500) have been experimentally demonstrated in a pillar-based PhC cavity [27], although with large V_{eff}. Finally, optimization of TM-like cavity modes in pillar-based structures might be useful for applications in which the active medium has well defined polarization properties, i.e. orthogonal to the PhC lattice plane.

In this paper, we propose and design efficient active devices for Si technology, by assuming the slot geometry and material properties already employed in previous works [12,13]. In particular, we combine planar slot waveguide confinement with cavity designs for high-Q TM-like modes (whose electric field is orthogonal to the slot interfaces), which is the main novelty of the present work. The procedure is as follows: we first optimize pillar-based PhC cavities in order to find a range of parameters for high-Q TM-like cavity modes, then we introduce a horizontal slot in the pillars and calculate the effective mode volume for the optimized structure, and finally we evaluate the expected Purcell factor.

2. Theoretical modeling

Pillar-based PhC structures are schematically represented in Fig. 1. The pillars are made of a high-dielectric constant material (Si), and are embedded in a medium with lower dielectric constant. Typically, the pillars are grown on an insulating substrate (e.g., SiO_2), and then infiltrated with a medium having a dielectric constant close to $\varepsilon_{\mathrm{clad}}$ [22]. This can be done, e.g., using flowable oxide (FOX) [28]. We focus on a square lattice with pillar radius r, in which a linear waveguide is defined by modifying to r_{def} the radii of an ideally infinite row of pillars (an L∞ defect according to our definition). A resonant cavity (point defect) can be obtained by modifying to r_{def} the radii of n pillars along the x (or y) direction: the point-defect is named "Ln" (e.g., an L11 cavity is shown in the figure). In general, defect modes

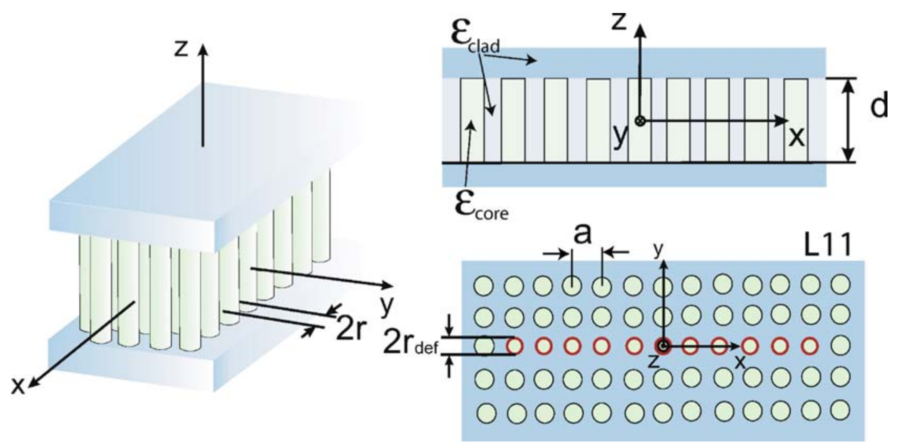

Fig. 1. System under consideration: lattice of pillars with period a, pillar radius r, pillar thickness d. The pillars ($\varepsilon_{\mathrm{core}} = 12$) are embedded in an insulating medium ($\varepsilon_{\mathrm{clad}} = 2.1$). Ln defect cavities are defined by changing to r_{def} the radius of n pillars along the x (or y) direction.

can be acceptor- or donor-like (following the solid-state nomenclature), depending on $r_{\mathrm{def}} < r$ or $r_{\mathrm{def}} > r$, respectively.

For the numerical treatment of such structures, we employ a guided-mode expansion (GME) method [29] allowing to perform a systematic modeling of the system as a function of its relevant system parameters. The GME method allows the accurate and quite fast calculation of both real (dispersion) and imaginary (losses) parts of the photonic eigenmodes. Losses are calculated by perturbation theory [29,30] and the quality factor is defined as

$$Q = \frac{\langle Re(\omega_{\mathrm{d}}(\mathbf{k}))\rangle}{2\langle Im(\omega_{\mathrm{d}}(\mathbf{k}))\rangle}, \quad (1)$$

where a supercell is used to calculate the defect mode complex dispersion $\omega_{\mathrm{d}}(\mathbf{k})$. The cavity mode Q-factor is derived after averaging over the $\mathbf{k}$-points in the first Brillouin zone of the superlattice [29]. This method has been used in a number of previous works, also showing a very good agreement with experiments both in one- [31], and two-dimensional [32–34] PhC cavities. For the calculations presented in this work, we used supercell sizes up to $18a \times 8a$, and up to 4000 plane waves in the GME basis. We only keep one guided mode in the basis for the expansion, which is justified as far as we restrict our attention to a range below the second-order mode cut-off. Convergence of the mode resonances and Q-factors with the number of plane waves has been checked.

The spontaneous emission rate of a dipolar emitter can be enhanced or inhibited by changing its surrounding electromagnetic environment. The Purcell factor F_P is a measure of the ratio between the spontaneous emission rate of the emitter in a cavity vs. the one in the bulk medium. For a dipole placed in the field antinode and perfectly aligned with the electric field, the Purcell factor can be expressed as [7,5]

$$F_P = \frac{6}{\pi^2}\frac{Q}{V_{\mathrm{a}}}, \quad (2)$$

where a dimensionless mode volume has been defined as [19]

$$V_{\mathrm{a}} = V_{\mathrm{eff}}\left(\frac{2\sqrt{\varepsilon(\mathbf{r}_{\max})}}{\lambda_{\mathrm{d}}}\right)^3, \quad (3)$$

and the effective mode volume is

$$V_{\mathrm{eff}} = \frac{\int \varepsilon(\mathbf{r})|\mathbf{E}(\mathbf{r})|^2 \mathrm{d}\mathbf{r}}{\max\{\varepsilon(\mathbf{r})|\mathbf{E}(\mathbf{r})|^2\}}. \quad (4)$$

3. Design of pillar-based cavities

It is reasonable to assume that a high-Q cavity mode can be obtained by properly discretizing the dispersion of a line-defect mode in a region of low losses. In Fig. 2(a) we show the calculated mode dispersion for an acceptor-like L∞ propagating mode of TM-like symmetry, for two different r_{def} values. Acceptor-like modes are generally found to display lower losses than donor-like ones [35]. The pillars height has been chosen from the maximization of the photonic band gap width

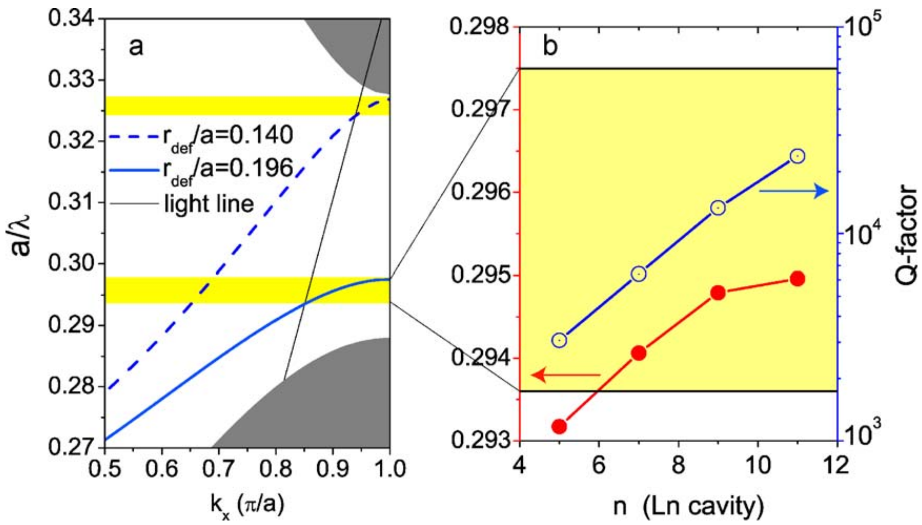

Fig. 2. (a) Guided mode dispersions calculated for acceptor-like line defects with two different defect pillars radii, while $r/a = 0.23$ and $d/a = 1.75$ are fixed. Low-loss frequency regions below the light line are highlighted. (b) Resonance frequency and corresponding Q-factor for Ln defect modes with $r_{\mathrm{def}}/a = 0.196$, as a function of the number of defect pillars, n. The low-loss region of the corresponding guided mode ("L∞" defect) is indicated.

on the fundamental TM-like modes. The highlighted region is the one below the cladding light line, where intrinsic diffraction losses are forbidden and the mode Q-factor is solely determined by disorder [24]. It can be seen in Fig. 2(b) that the confined modes of Ln cavities display increasing Q-factors on increasing number n of defect rods. In other words, higher Q-factors are obtained when the cavity mode frequency approaches the band edge of the propagating line-defect mode, thereby confirming the starting assumption. For an acceptor-like L11 cavity we find $Q \simeq 24000$. As it can be expected, on increasing the number of defect rods the Q-factor increases, slowly converging towards its limiting value in the waveguide mode for $n \to \infty$. Although, the mode volume and disorder-induced losses would increase as well on approaching the slow-light region of the propagating defect mode [24], thus hindering the maximum Q-factor that could realistically be achieved. We conclude that a L11 cavity represents a reasonable compromise between having large Q and small $V_{\rm eff}$ for CQED applications.

To achieve a further optimization of such value, we perform a systematic analysis as a function of shifting and shrinking of nearby pillars parameters, following a local geometry optimization approach already employed for hole-based PhC cavities [3]. We report in Fig. 3(a) the results of the L11 cavity mode resonant frequency and Q-factor, respectively, as a function of nearby pillars shift, Δx. We find a maximum $Q \simeq 34000$ for $\Delta x/a = -0.1$. For such structure parameters, we further optimize the Q-factor by changing the nearby pillars' radii, as shown in Fig. 3(b). The maximum theoretical $Q \simeq 45000$ is found for $\Delta r/a = -0.01$ (i.e. slightly smaller pillars).

4. Purcell factor in slotted pillar cavities

The introduction of a low-index slot in the pillars center, as schematically shown in Fig. 4, is expected

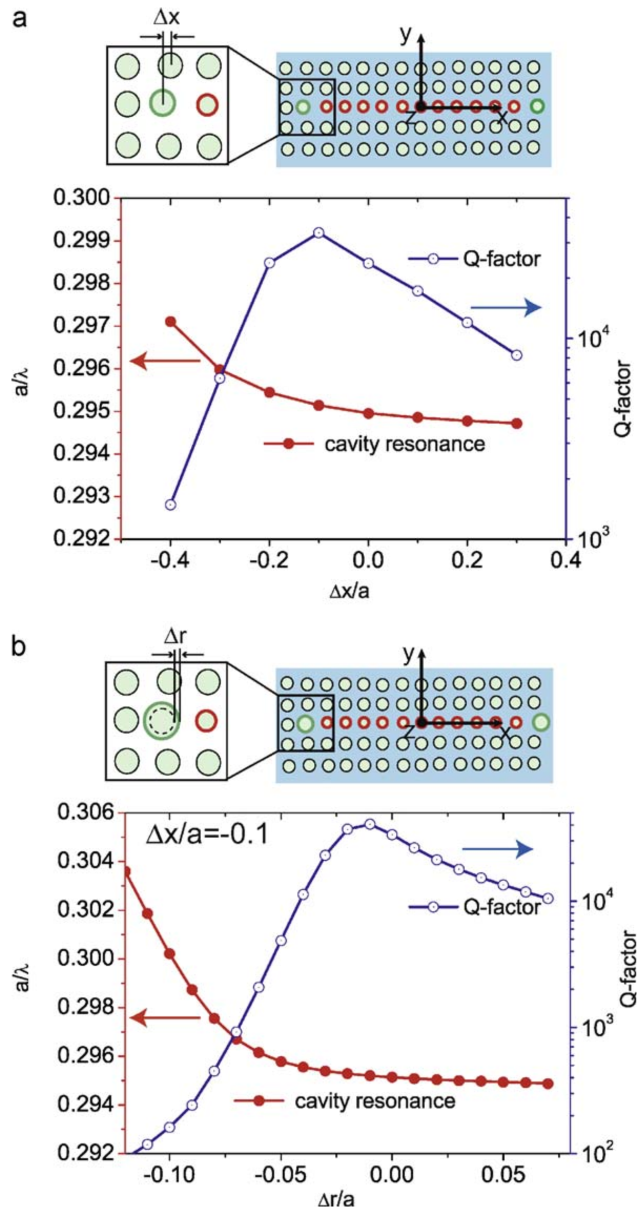

Fig. 3. Q-factor optimization of L11 pillar cavity (without slot): (a) as a function of nearby pillars shift along the line defect direction, Δx, and (b) as a function of modified radius of the same pillars, Δr, for fixed $\Delta x/a = -0.1$ (which maximizes Q).

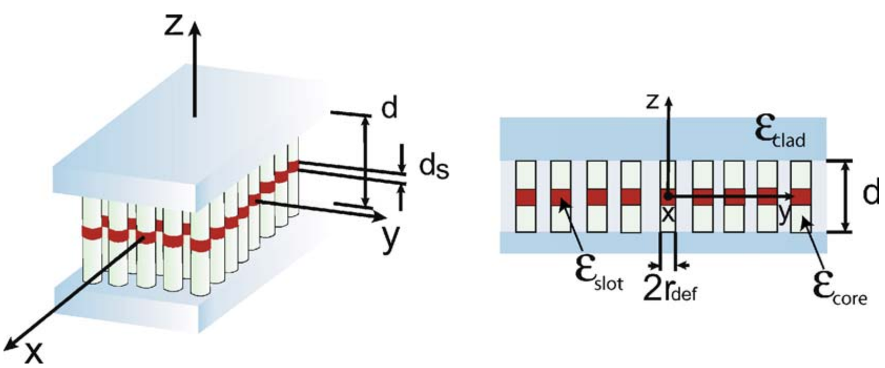

Fig. 4. A low-index slot ($\varepsilon_{\rm slot} = 2.89$) of thickness $d_{\rm s}$ is included within the rods. The other parameters of the systems are defined as in Fig. 1.

to reduce the Q-factor. On the other hand, a concentration of the field in the slot brings a reduction in mode volume as well, thus maximizing the Purcell factor. Considering the L11-type cavity optimized above, with $\Delta x/a = -0.1$ and $\Delta r/a = -0.01$, we introduce a slot of thickness $d_s/a = 0.05$ and dielectric constant 2.89 (appropriate, in general, for a Si-rich oxide layer). These values are consistent with previously fabricated samples [12,13] in which the active slot is made of Er-doped SiO_2. An optimization of the slot thickness has been recently studied in [36]. To simulate this structure, we employ an extension of the GME method to multilayer vertical dielectric structures, in which the basis of guided modes for the expansion is found by numerically applying the transfer matrix method. We use 4005 plane waves in the expansion, which are sufficient for convergence of both real and imaginary parts of cavity mode eigenvalues. Given that we are below the second-order TM-like mode, only one guided mode is kept in the expansion, but we checked that no appreciable change would be obtained by keeping two guided modes in the basis. A color plot of the calculated cavity mode (the field is normalized such that $\int \varepsilon(\mathbf{r})|\mathbf{E}(\mathbf{r})|^2 d\mathbf{r} = 1$) is given in Fig. 5(a), showing the field enhancement in the low-index slot. A direct comparison of the vertical field profiles for the structure with and without slot, respectively, is shown in Fig. 5(b). In the latter, the field profile only depends on the index contrast between the slot and the surrounding medium constituting the rods, and thus it can be qualitatively extended to the other rods as well. The dimensionless mode volume V_a is reduced by a factor of 3 with respect to the structure without slot, while the Q-factor is still quite large ($Q \simeq 30000$ and $V_a \simeq 1.1$ for this structure). As a consequence, the Purcell factor is predicted to reach $F_P \simeq 15000$ in our optimized slot structure. For comparison, the F_P value that can be obtained in a L11 cavity without slot is ~8000, about a factor of 2 smaller. In fact, even if the Q-factor is larger in the structure without slot, the increased mode volume leads to a smaller Purcell enhancement factor, as derived from Eq. (2).

We have made a further systematic analysis and calculated the corresponding figures of merit also for other cavity structures. In particular, for the acceptor-like modes we have also considered the L9-type cavity, and for the donor-like defect modes we have optimized the L7- and L9-type structures, respectively, along the lines reported in the previous section (results not shown). The comparison is summarized in Table 1. As it can be seen, the L11-type cavity is the one showing the best Purcell enhancement as a consequence of the optimized Q-factor for the corresponding pillar-based structure.

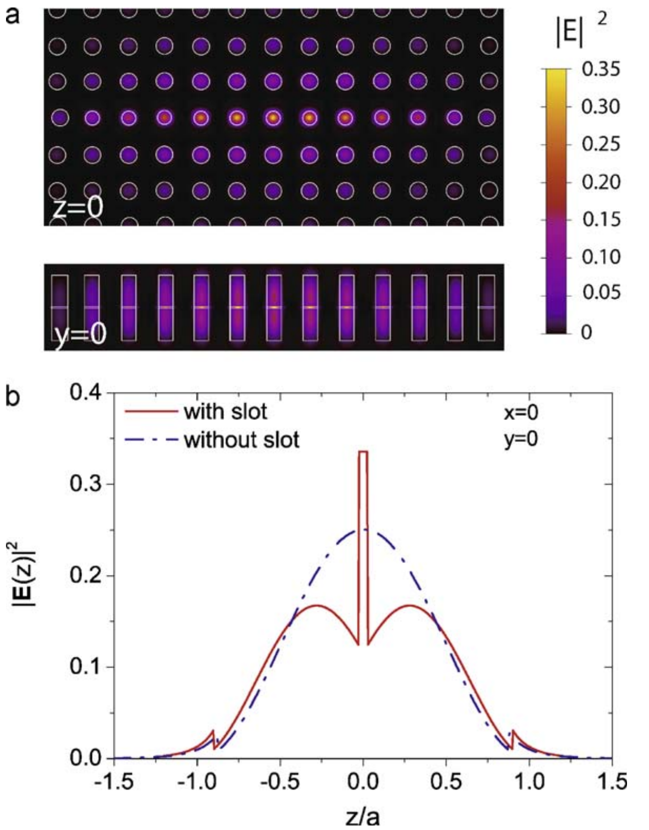

Fig. 5. (a) Normalized field intensity profile for the optimized L11 cavity mode (i.e. $\Delta x/a = -0.1$, $\Delta r/a = -0.01$) with slotted pillars ($d_s/a = 0.05$, total rod thickness $d/a = 1.8$) in the (x,y) and (x,z) planes, respectively. (b) Field intensity along z for $x = y = 0$, i.e. along the central pillar of the cavity. For comparison, the field intensity profile is also shown for the case without slot (rod thickness $d/a = 1.75$).

In summary, we have shown that an enhancement of spontaneous emission rate on the order of $\sim 10^4$ can be achieved in Si-based cavities made of slotted pillars, meant to be fabricated with a low-index Er-doped Si dioxide slot in the pillars center as an active

Table 1
Defect pillar radius, cavity-type and corresponding Q-factor and dimensionless mode volume for slotted pillars with $d_S/a = 0.05$. In the last column the Purcell factor is reported for a single emitter placed at the field antinode in each structure.

r_{def}/a	Cavity-type	Q	V_a	F_P
0.196	L9	$\simeq 1.26 \times 10^4$	$\simeq 1.02$	$\simeq 7.5 \times 10^3$
0.196	L11	$\simeq 2.75 \times 10^4$	$\simeq 1.08$	$\simeq 1.5 \times 10^4$
0.322	L7	$\simeq 4.9 \times 10^3$	$\simeq 0.79$	$\simeq 3.8 \times 10^3$
0.322	L9	$\simeq 7 \times 10^3$	$\simeq 0.97$	$\simeq 4.4 \times 10^3$

medium. Considering an operational wavelength $\lambda_d = 1.55$ μm, i.e. around the Er emission band, the lattice constant should be $a \simeq 460$ nm, with a rod height $d \simeq 800$ nm and a slot thickness $d_s \simeq 25$ nm for the optimal structure parameters found in this work. Such structure is readily realizable within current Si-based fabrication technology, and this suggests applications of the present results for CMOS-compatible light emitting devices at telecom wavelengths to be integrated on a chip.

5. Conclusions

We have performed a systematic computational analysis of pillar-based photonic crystal cavities in square lattice, with the aim of optimizing the Q/V_{eff} figure of merit in planar slot waveguides for cavity QED applications. We have shown that acceptor-like defect mode with TM polarization are generally more suited to achieve large Q-factor and small mode volume in slotted pillars structures. As a result, we have reported structure parameters for L11-type cavities that can readily be realized in silicon-based light emitting devices whose active medium is made of enriched Si dioxide.

Acknowledgement

This project was supported by MIUR through FAR project n. 851 ‘‘Si-based lasers and optical amplifiers’’.

References

[1] J.D. Joannopoulos, S.G. Johnson, J.N. Winn, R.D. Meade, Photonic Crystals: Molding the Flow of Light, Princeton University Press, Princeton, 2008.
[2] S.G. Johnson, S. Fan, P.R. Villeneuve, J.D. Joannopoulos, L.A. Kolodziejski, Guided modes in photonic crystal slabs, Phys. Rev. B 60 (1999) 5751.
[3] Y. Akahane, T. Asano, B.S. Song, S. Noda, High-Q photonic nanocavity in a two-dimensional photonic crystal, Nature (London) 425 (2003) 944.
[4] E. Kuramochi, M. Notomi, S. Mitsugi, A. Shinya, T. Tanabe, T. Watanabe, Ultrahigh-Q photonic crystal nanocavities realized by the local width modulation of a line defect, Appl. Phys. Lett. 88 (2006) 041112.
[5] L.C. Andreani, G. Panzarini, J.-M. Gérard, Strong coupling regime for quantum boxes in pillar microcavities: theory, Phys. Rev. B 60 (1999) 13276.
[6] J. Vučković, M. Lončar, H. Mabuchi, A. Scherer, Design of photonic crystal microcavities for cavity QED, Phys. Rev. E 65 (2001) 016608.
[7] E.M. Purcell, Spontaneous emission probabilities at radio frequencies, Phys. Rev. 69 (1946) 681.
[8] A. Badolato, K. Hennessy, M. Atatüre, J. Dreiser, E. Hu, P.M. Petroff, A. Imamoğlu, Deterministic coupling of single quantum dots to single nanocavity modes, Science 308 (2005) 1158.
[9] D. Englund, D. Fattal, E. Waks, G. Solomon, B. Zhang, T. Nakaoka, Y. Arakawa, Y. Yamamoto, J. Vučković, Controlling the spontaneous emission rate of single quantum dots in a two-dimensional photonic crystal, Phys. Rev. Lett. 95 (2005) 013904.
[10] M. Toishi, D. Englund, A. Faraon, J. Vučković, High-brightness single photon source from a quantum dot in a directional emission nanocavity, Opt. Express 17 (2009) 14618.
[11] G.T. Reed, Silicon Photonics: The State of the Art, Wiley, Chichester, 2008.
[12] M. Galli, A. Politi, M. Belotti, D. Gerace, M. Liscidini, M. Patrini, L.C. Andreani, M. Miritello, A. Irrera, F. Priolo, Y. Chen, Strong enhancement of Er^{3+} emission at room temperature in silicon-on-insulator photonic crystal waveguides, Appl. Phys. Lett. 88 (2006) 251114.
[13] C. Creatore, L.C. Andreani, M. Miritello, R. Lo Savio, F. Priolo, Modification of erbium radiative lifetime in planar silicon slot waveguide, Appl. Phys. Lett. 94 (2009) 103112.
[14] V.R. Almeida, Q. Xu, C.A. Barrios, M. Lipson, Ultracompact guiding and confining light in void nanostructure, Opt. Lett. 29 (2004) 1209.
[15] Q. Xu, V.R. Almeida, R.R. Panepucci, M. Lipson, Experimental demonstration of guiding and confining light in nanometer-size low-refractive-index material, Opt. Lett. 29 (2004) 1626.
[16] M. Galli, D. Gerace, A. Politi, M. Liscidini, M. Patrini, L.C. Andreani, A. Canino, M. Miritello, R. Lo Savio, A. Irrera, F. Priolo, Direct evidence of light confinement and emission enhancement in active silicon-on-insulator slot waveguides, Appl. Phys. Lett. 89 (2006) 241114.
[17] R. Sun, P. Dong, N.-N. Feng, C.-Y. Hong, J. Michel, M. Lipson, L. Kimerling, Horizontal single and multiple slot waveguides: optical transmission at $\lambda = 1550$ nm, Opt. Express 15 (2007) 17967.
[18] A. Di Falco, L. O'Faolain, T.F. Krauss, Dispersion control and slow light in slotted photonic crystal waveguides, Appl. Phys. Lett. 92 (2008) 083501.
[19] J.T. Robinson, C. Manolatou, L. Chen, M. Lipson, Ultrasmall mode volumes in dielectric optical microcavities, Phys. Rev. Lett. 95 (2005) 143901.
[20] S.-H. Kwon, T. Sünner, M. Kamp, A. Forchel, Optimization of photonic crystal cavity for chemical sensing, Opt. Express 16 (2008) 11709.
[21] T. Yamamoto, M. Notomi, H. Taniyama, E. Kuramochi, Y. Yoshikawa, Y. Torii, T. Kuga, Design of a high-Q air-slot cavity based on a width-modulated line-defect in a photonic crystal slab, Opt. Express 16 (2008) 13809.
[22] M. Tokushima, H. Yamada, Y. Arakawa, 1.5-μm wavelength light guiding in waveguides in square lattice of rod photonic crystal slabs, Appl. Phys. Lett. 84 (2004) 4298.
[23] S. Assefa, P.T. Rakich, P. Bienstman, S.G. Johnson, G.S. Petrich, J.D. Joannopoulos, L.A. Kolodziejski, E.P. Ippen, H.I. Smith, Guiding 1.5-μm light photonic crystals based on dielectric rods, Appl. Phys. Lett. 85 (2004) 6110.
[24] D. Gerace, L.C. Andreani, Effects of disorder on propagation losses and cavity Q-factors in photonics crystal slabs, Photonics and Nanostructures, Fundam. Appl. 3 (2005) 120.
[25] H. Zhang, L.A. Dunbar, G. Scalari, R. Houdré, J. Faist, Terahertz photonic crystal quantum cascade lasers, Opt. Express 15 (2007) 16818.
[26] L. Ferrier, O. El Daif, X. Letartre, P. Rojo Romeo, C. Seassal, R. Mazurczyk, P. Viktorovitch, Surface emitting microlaser based on 2D photonic crystal rod lattices, Opt. Express 17 (2009) 9780.

[27] T. Xu, N. Zhu, M.Y.-H. Xu, L. Wosinski, J.S. Aitchison, H.E. Ruda, A pillar-array based two-dimensional photonic crystal microcavity, Appl. Phys. Lett. 94 (2009) 241110.
[28] T.P. White, L. O'Faolain, J. Li, L.C. Andreani, T.F. Krauss, Silica-embedded silicon photonic crystal waveguides, Opt. Express 16 (2008) 17076.
[29] L.C. Andreani, D. Gerace, Photonic crystal slabs with a triangular lattice of triangular holes investigated using a guided-mode expansion method, Phys. Rev. B 73 (2006) 235114.
[30] T. Ochiai, K. Sakoda, Nearly free-photon approximation for two-dimensional photonic crystal slabs, Phys. Rev. B 64 (2001) 045108.
[31] D. Gerace, M. Galli, D. Bajoni, G. Guizzetti, L.C. Andreani, F. Riboli, M. Melchiorri, N. Daldosso, L. Pavesi, G. Pucker, S. Cabrini, L. Businaro, E. Di Fabrizio, Wide-band transmittance of one-dimensional photonic crystals carved in Si_3N_4/SiO_2 channel waveguides, Appl. Phys. Lett. 87 (2005) 211116.
[32] A.R.A. Chalcraft, S. Lam, D. O'Brien, T.F. Krauss, M. Sahin, D. Szymanski, D. Sanvitto, R. Oulton, M.S. Skolnick, A.M. Fox, D.M. Whittaker, H.-Y. Liu, M. Hopkinson, Mode structure of the L3 photonic crystal cavity, Appl. Phys. Lett. 90 (2007) 241117.
[33] M. Galli, S.L. Portalupi, M. Belotti, L.C. Andreani, L. O'Faolain, T.F. Krauss, Light scattering and Fano resonances in high-Q photonic crystal nanocavities, Appl. Phys. Lett. 94 (2009) 071101.
[34] S.L. Portalupi, M. Galli, C. Reardon, T.F. Krauss, L. O'Faolain, L.C. Andreani, D. Gerace, Planar photonic crystal cavities with far-field optimization for high coupling efficiency and quality factor, Opt. Express 18 (2010) 16064.
[35] H. Benisty, D. Labilloy, C. Weisbuch, C.J.M. Smith, T.F. Krauss, D. Cassagne, A. Béraud, C. Jouanin, Radiation losses of waveguide-based two-dimensional photonic crystals: positive role of the substrate, Appl. Phys. Lett. 76 (2000) 532.
[36] Y.C. Jun, R.M. Briggs, H.A. Atwater, M.L. Brongersma, Broadband enhancement of light emission in silicon slot waveguides, Opt. Express 17 (2009) 7479.